Phase transition drives bacterial single-stranded DNA binding (SSB) protein mobilization during stress response and metabolic adaptation

Péter Ecsédi[1], Júlia Szittyai[1], János Pálinkás[1,2], Bálint Jezsó[1,2], Viktoria Katran[1], Zoltán J. Kovács[1,2], Henriett Halász[3], Tasvilla Sonallya[4], Tünde Juhász[4], Tamás Beke-Somfai[4], Szilvia Barkó[3], Edina Szabó-Meleg[3], and Mihály Kovács[1,2*]

[1] ELTE-MTA "Momentum" Motor Enzymology Research Group, Department of Biochemistry, Eötvös Loránd University, H-1117 Budapest, Hungary
[2] HUN-REN-ELTE Motor Pharmacology Research Group, Department of Biochemistry, Eötvös Loránd University, H-1117 Budapest, Hungary
[3] Department of Biophysics, Medical School, University of Pécs, H-7624 Pécs, Hungary
[4] Institute of Materials and Environmental Chemistry, HUN-REN Research Centre for Natural Sciences, Budapest H-1117, Hungary

* Correspondence: mihaly.kovacs@ttk.elte.hu

Keywords: Super-resolution imaging, single-stranded DNA binding protein (SSB), liquid-liquid phase separation (LLPS), stress response, DNA repair, metabolism

Abstract

Single-stranded DNA-binding proteins (SSBs) are ubiquitous factors of genome metabolism, recently recognized for their ability to undergo liquid–liquid phase separation (LLPS). While *Escherichia coli* SSB (EcSSB) has emerged as a model for bacterial LLPS *in vitro*, its phase behavior and functional dynamics *in vivo* have remained largely unexplored. Here, we define the subcellular organization of EcSSB under diverse physiological and stress conditions using super-resolution microscopy coupled with newly developed image analysis tools. We demonstrate that EcSSB forms dynamic condensates during exponential growth, which disassemble in response to DNA damage, oxidative stress, antibiotic exposure, and metabolic adaptation. These phase transitions are attenuated in stationary-phase cells, indicative of reduced responsiveness. Moreover, we show that EcSSB is spatially segregated from nucleoid regions under stress-free conditions, but relocalizes to DNA-rich regions upon stress induction, supporting a regulated condensate-to-function transition. Our findings provide direct *in vivo* evidence for stress- and growth-phase-dependent modulation of EcSSB phase behavior, corroborated by biophysical characterization of EcSSB condensates bridging *in vitro* observations with physiological relevance. Our work establishes a quantitative framework for dissecting LLPS dynamics in bacterial cells and sets the stage for future strategies to target condensate-regulated pathways in antimicrobial development.

Significance statement

We demonstrate *in vivo* that the *Escherichia coli* single-stranded DNA-binding protein (EcSSB) forms liquid–liquid phase-separated condensates during normal growth that rapidly dissolve upon DNA damage, oxidative, or metabolic stress, enabling swift relocalization to DNA. These results establish LLPS as a tunable mechanism for macromolecular sequestration and mobilization in bacteria, bridging *in vitro* observations with physiological function. Moreover, EcSSB condensation appears to confer a selective advantage under fluctuating conditions, highlighting phase separation as a potential target for antimicrobial development.

Introduction

Living cells must respond rapidly and effectively to DNA damage to mitigate its potentially severe impacts. Among others, ionizing and ultraviolet radiation, alkylating agents, and polycyclic aromatic hydrocarbons can cause exogenous DNA damage [1]. In addition, DNA is also vulnerable during physiological DNA metabolic processes including DNA replication, recombination, and repair. Nearly all genome maintenance pathways involve exposure of single-stranded DNA (ssDNA) segments whose processing is mediated by the action of single-stranded DNA binding (SSB) proteins in both prokaryotic and eukaryotic cells [2].

SSBs protect ssDNA from degradation and prevent its reannealing. In addition, SSBs recruit and organize genome maintenance complexes through protein–protein interactions (PPIs) [2]. *Escherichia coli* SSB (EcSSB), the prototypic SSB, is a homotetramer of 178-amino acid (19-kDa) subunits [3]. An EcSSB subunit comprises the N-terminal globular oligonucleotide/oligosaccharide-binding (OB) domain (amino acids (aa) 1-113) responsible for ssDNA binding [4], and an intrinsically disordered linker (IDL, aa 114-178) driving PPIs [5,6]. The C-terminal segment of the IDL (so-called C-terminal peptide, CTP, aa 170-178), a key PPI element, is highly conserved among bacteria [2,3,5,7,8]. It was recently demonstrated that EcSSB liquid-liquid phase separation (LLPS) is brought about by a fine-tuned interplay of the protein's different structural regions [9-11].

LLPS of proteins has been known for more than a century, yet its biological importance has only been recently recognized [12-15]. Numerous proteins have been reported to be capable of LLPS-based condensation [12,16], and LLPS has emerged as a key mechanism for the formation of membraneless organelles [17,18]. Examples for these structures in eukaryotes include Cajal bodies, P granules, and the nucleolus [15]. The formation of LLPS particles is typically driven by weak multivalent protein-protein and/or protein-nucleic acid interactions [19,20]. LLPS condensates serve a wide range of functions, such as buffering concentrations of proteins, rapid mobilization of biomolecules upon stress, and enhancing reactions by selectively concentrating molecules involved in biochemical processes [21,22]. Although the role of protein condensation in bacteria has remained less explored, it has recently become increasingly apparent that this phenomenon bears special importance within the spatial confines of bacterial cells lacking internal membrane-based compartmentalization [12,21]

The above recognition aligns with our previous *in vitro* finding that increasing concentrations of ssDNA dissolve EcSSB condensates in a stoichiometric fashion, suggesting a role for dynamic EcSSB decondensation in bacterial genome maintenance [9]. However, a comprehensive *in vivo* analysis of EcSSB condensate behavior has been lacking. A main challenge in studying bacterial condensates is the difficulty of visualization at this scale. Using super-resolution microscopy, Zhao *et al.* assessed the intracellular localization of EcSSB using an *E. coli* strain expressing a GFP-fused EcSSB variant from a genomic locus [23]. In unstressed state, EcSSB foci localized near the membrane and, to a lesser extent, at genomic sites. Treatment with the DNA damaging agent mitomycin C triggered the dissociation of EcSSB from the membrane, with nearly all EcSSB being found inside the cell. These indications, together with the ssDNA-gated *in vitro* condensation features of EcSSB [9-11,24], motivated us to perform a comprehensive definition of EcSSB subcellular patterns during bacterial growth, stress responses, and metabolic adaptations.

In this work, we combine super-resolution microscopy and quantitative image analysis to provide *in vivo* evidence that EcSSB forms condensates in the cell and that these phase-separated structures undergo stress- and growth-phase-dependent remodeling, correlating with DNA damage, metabolic state, and proliferation cues. Our results support that SSB condensation

contributes to cytoplasmic phase transitions and provides bacteria with a tunable way to modulate macromolecular mobility, sequestration, and release.

Results

EcSSB forms dynamic condensates during growth, which consolidate upon growth arrest

To define the condensation behavior of EcSSB during bacterial growth, we recorded subcellular EcSSB patterns in exponential, stationary, and late ("death") growth phases using a well-characterized *E. coli* strain (#29003) expressing EcSSB-GFP alongside the wild-type protein **(Fig. 1 and Table S1)** [23]. Importantly, the sequence encoding EcSSB-GFP was introduced downstream—not in place—of the wild-type (WT) EcSSB coding sequence in this strain. Consequently, these bacteria express both WT EcSSB and a smaller fraction of EcSSB-GFP without induction. Previously it was shown that, under these conditions, both WT and chimeric SSB tetramers can form, with the latter retaining WT activity even when the tetramer contains up to two GFP-fused subunits [25]. Thus, the fused construct can be utilized for fluorescence-based detection, while the WT protein provides intact SSB functionality in the cells [23].

In the early exponential phase (OD_{600} = 0.2), cells exhibited weak EcSSB-GFP signals, with few faint foci observed. The low signal intensity was likely due to low protein expression and/or GFP maturation levels at this stage [26]. The majority of EcSSB condensates (typically 1, but up to 6, per cell) appeared in the exponential phase (OD_{600} = 0.6). Notably, in late exponential and early stationary phases (OD_{600} = 0.6 + 1.5 h, + 3 h, and + 4.5 h), the number of droplets in cells tended to consolidate into a single droplet, with cells lacking condensates becoming exceedingly rare. This trend shifted in later phases (OD_{600} = 0.6 + 7 h, + 10 h, and + 24 h) toward the dissolution of EcSSB assemblies. During these stages, the overall EcSSB-GFP signal diminished, indicating the onset of long-term stationary phase and cell death [27,28].

The time-dependent trend in EcSSB-GFP condensate signal intensity indicates that the appearance of more intense droplets is associated with reduced rates of division and correspondingly slower metabolism (*e.g.* OD_{600} = 0.6 compared to OD_{600} = 0.6 + 3 h, **Fig. 1**). Furthermore, as the number of droplets decreased, their intensity increased, reflecting fusion of smaller condensates into a larger assembly (condensate maturation/coalescence; see also *in vitro* biophysical evidence described below). Based on EcSSB-GFP signal intensity analysis including all cells either harboring or lacking droplets, we detected a reduction in diffuse cytoplasmic EcSSB-GFP signal as cultures grew older, further indicating the assimilation of the dissolved EcSSB pool into condensates (eventually, up to 70 % of the total EcSSB-GFP signal became localized in condensate droplets) (**Fig. 1** and **Fig. S1**). We note that the high proportion of the cellular EcSSB-GFP signal in the condensate form is also indicative of efficient incorporation of EcSSB-GFP into endogenous (wild-type) EcSSB droplets. During the death phase (OD_{600} = 0.6 + 10 h and 24 h), the overall cellular EcSSB-GFP signal declined, ultimately leading to the complete disappearance of droplets. Taken together, these observations provide evidence for our earlier proposition that EcSSB condensates act as protein reservoirs *in vivo*, sequestering EcSSB and likely its protein partners [9,24].

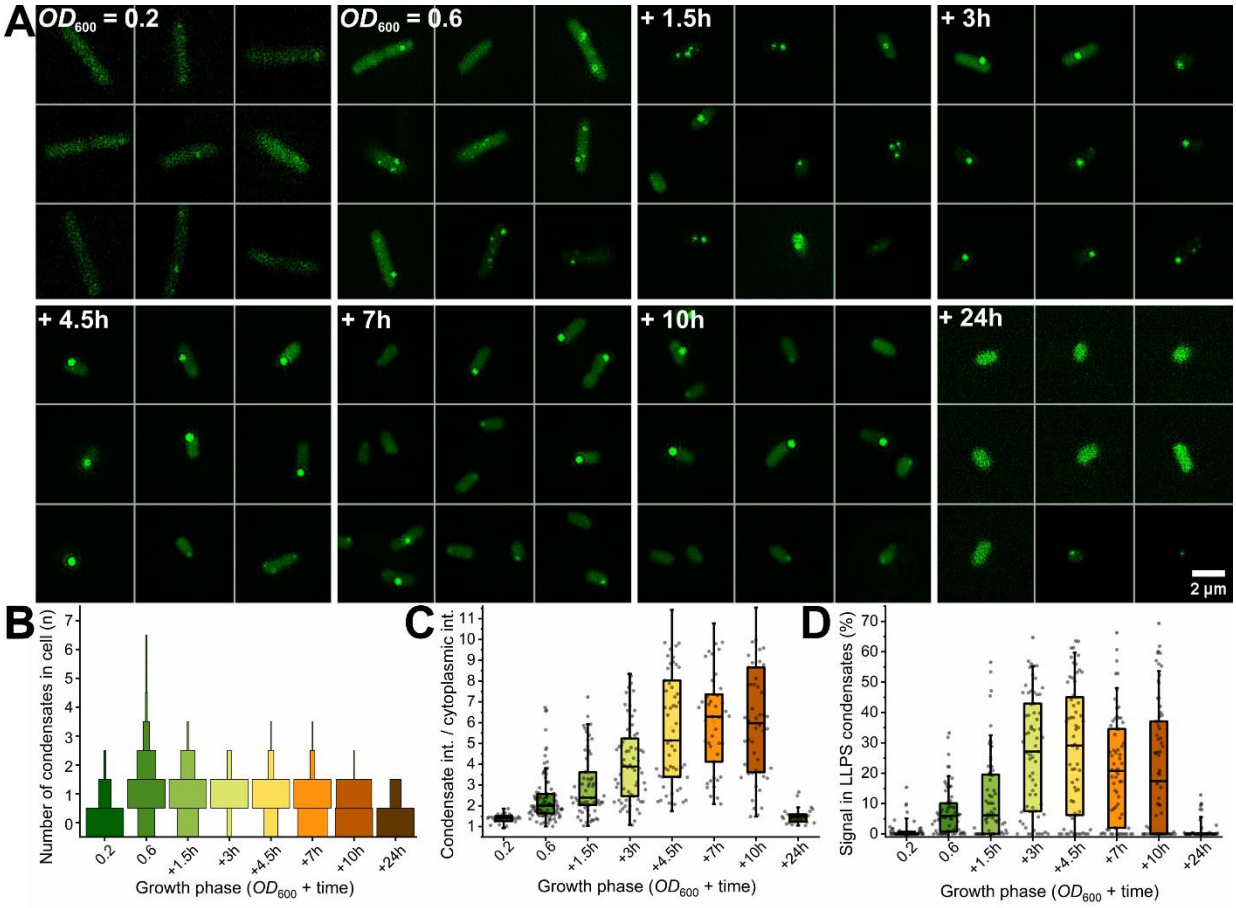

Figure 1. EcSSB shows gradual accumulation within cells during bacterial growth. (A) *Structured illumination microscopic (SIM) images of the EcSSB-GFP-expressing E. coli strain #29003* [23] *in different growth phases. Images were evaluated using a newly developed analysis methods described in* ***Supplementary file 1****. Data showing* ***(B)*** *the number of condensates per cell,* ***(C)*** *condensate intensities, and* ***(D)*** *the percentage of signal in condensates reveal successive accumulation of EcSSB from multiple droplets into a single droplet during cell growth (n = 65 cells analyzed per condition, see also* ***Table S1****).*

EcSSB condensates disassemble under stress, but this process is attenuated in stationary-phase cells

Next, we analyzed the effects of a broad panel of stressors and metabolic modulators (described in **Table S2**, including dosages and mechanisms of action) on cells in the exponential growth phase (OD_{600} = 0.6). Of the applied agents, (*i*) hydroxyurea (HU) and NaCl suppress, while (*ii*) L-arginine (L-Arg), glucose, and lactose stimulate cell growth; (*iii*) UV irradiation, nitrofurantoin, and methyl methanesulfonate (MMS) directly damage DNA; (*iv*) diamide and H_2O_2 cause different forms of oxidative stress; (*v*) myricetin and taxifolin are antibacterial flavonoids interacting with prokaryotic SSBs [29,30]; and (*vi*) MES (2-(N-morpholino)ethanesulfonic acid, pH 6) was used to cause pH stress. Importantly, most applied stressors induced a decrease in the number and intensity of EcSSB condensates, with a concomitant increase in cytoplasmic EcSSB-GFP signal (**Fig. 2 and Table S3**). UV, L-Arg, glucose, H_2O_2, MES pH 6, myricetin, and taxifolin exerted the strongest effects. Upon these treatments, the most frequently observed number of condensates dropped to 0 (except in case of H_2O_2). Moreover, with a few exceptions, stressed cells contained less than 5 % of the EcSSB-GFP signal (if any) in condensate form, in contrast to the typical 10-20 % (maximum 40 %) in untreated cells (**Fig. 2D**). Notably, glucose, which is a more favored energy source for *E. coli*

than lactose, exerted a more pronounced EcSSB decondensation effect compared to the sugar alternative (**Fig. 2 and Table S3**). Taken together, these results provide evidence for stress-induced and metabolic change-induced EcSSB decondensation, supporting our earlier proposition based on EcSSB's *in vitro* condensation features [9,11].

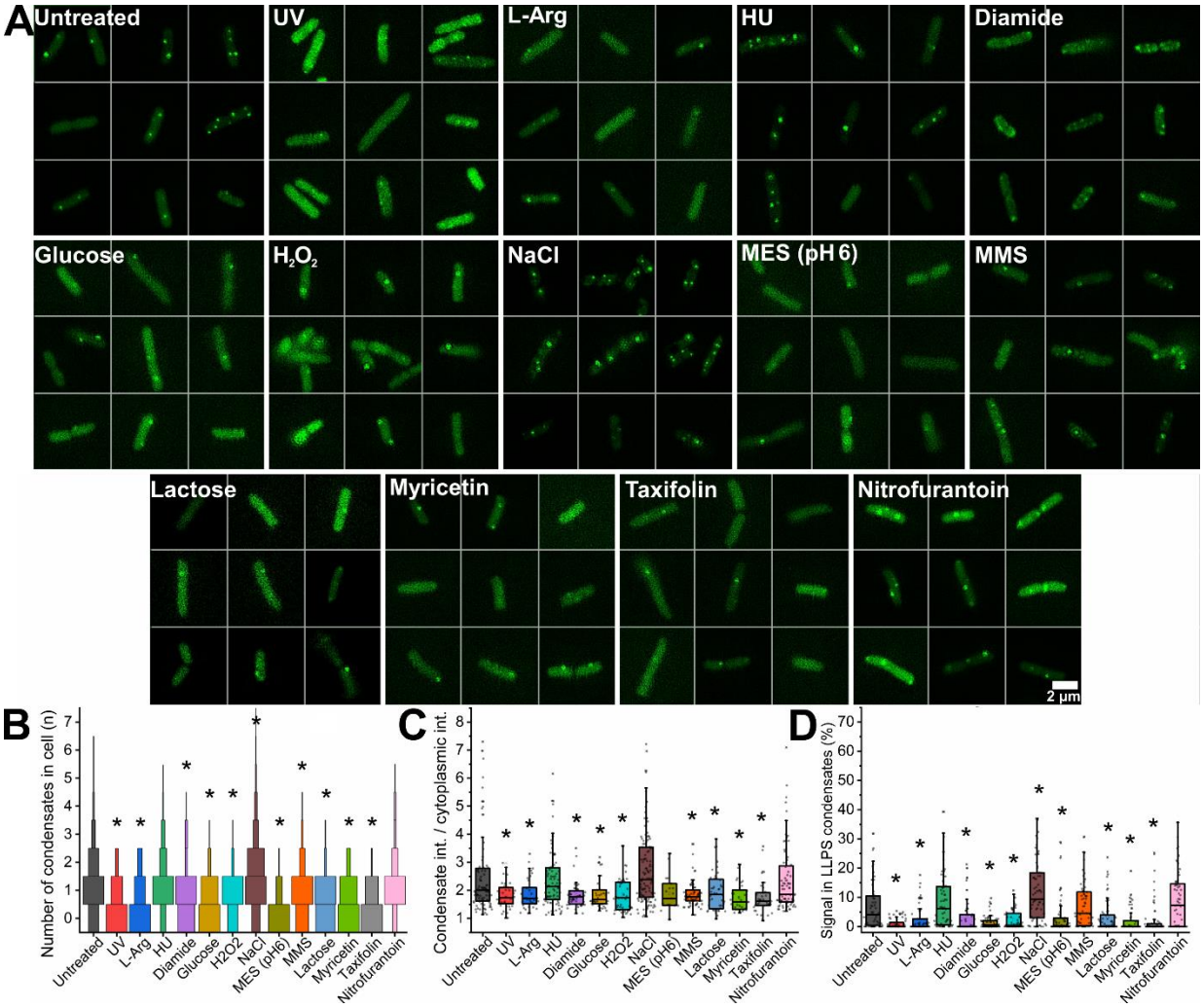

Figure 2. Various stressors induce EcSSB decondensation in exponential growth phase (OD_{600} = 0.6). (A) *Representative SIM images of E. coli strain #29003 show distinct EcSSB-GFP condensates in untreated cells. Upon exposure to various stressors (as indicated; see* ***Table S2*** *for conditions), the EcSSB-GFP signal became dispersed throughout the cytoplasm, while* ***(B)*** *the number and* ***(C)*** *intensity of foci decreased, indicating dissolution of EcSSB condensates.* ***(D)*** *The reduction in the percentage of signal in droplets further corroborates stress-induced condensate dissolution. Asterisks denote significant difference compared to untreated cells (Mann-Whitney test, $p < 0.05$, $n = 65$ cells analyzed per condition, see also* ***Table S3****).*

Other stressors including HU, MMS, nitrofurantoin, and NaCl, caused mild or no EcSSB decondensation effect (**Fig. 2 and Table S3**). Intriguingly, NaCl stress even enhanced EcSSB granulation, despite chloride ions being strong *in vitro* inhibitors of EcSSB condensation [9,11,24]. NaCl presumably causes osmotic changes in the cytoplasm, which could increase the local concentration of EcSSB, thereby driving condensate formation (see also biophysical results described below). HU was previously found to transiently inhibit DNA replication and repress DNA synthesis by dNTP depletion in *E. coli*, while the total amount of cellular DNA remained stagnant in the corresponding time period [31]. These effects can explain the lack of impact of HU on EcSSB condensation patterns, as replication stalling reduces ssDNA production;

consequently, existing EcSSB condensates remain stable, since no new ssDNA is generated to recruit EcSSB and alter their phase behavior (**Fig. 2 and Table S3**). The mild EcSSB decondensation effect of MMS could be due to the short exposure time applied [32,33]. Diamide had a special effect in causing EcSSB condensates to localize more toward the cell membrane, similar to that seen for untreated cells by Zhao *et al.* [23], in line with the observed interaction of EcSSB with membrane phospholipids in that study. Here we note that we also tested the effect of the FM 4-64 membrane dye, used by Zhao *et al.* [23], on EcSSB-GFP subcellular patterns. Intriguingly, we found that the dye caused EcSSB-GFP localization to membrane-adjacent cellular areas (**Figs. S2 E-G**), and therefore we refrained from its use in other experiments. The possibility that the membrane-associated green signal could originate from FM 4-64 fluorescence bleed-through can be excluded based on (*i*) the complete disappearance of EcSSB-GFP signal from internal cellular areas; (*ii*) the lack of the EcSSB-GFP membrane localization effect at lower FM 4-64 concentrations (2 μM, as used by Zhao *et al.*) with detectable red fluorescence; (*iii*) the occasional presence of red fluorescent spots (FM 4-64 aggregates) showing no signal in the green channel.

Next, we determined the effects of the above-mentioned stressors during the stationary and death phases (OD_{600} = 0.6 + 3h (**Fig. 3 and Table S4**), OD_{600} = 0.6 + 24 h (**Fig. S2 and Table S5**), respectively). In the stationary phase, stressors elicited generally milder responses compared to the exponential phase. Nevertheless, UV, L-Arg, glucose, H_2O_2, and MES (pH 6) still elicited effective, albeit partial, EcSSB condensate dissolution in these phases. At the same time, an increase in the diffuse cytoplasmic EcSSB-GFP signal, along with the fragmentation of protein condensates, was evident, as reflected by the appearance of more numerous, less intense droplets. Glucose, lactose and, notably, HU were exceptions, as these agents primarily increased the cytoplasmic signal without significant condensate fragmentation. We attribute these findings to the applied sugars gradually reactivating DNA metabolic processes requiring free EcSSB, with a slow transformation, and UV, H_2O_2, and MES (pH 6) inducing more rapid and more pronounced disassembly of EcSSB condensates, leading to condensate fragmentation. HU stands out as it exhibited no significant effect during the exponential phase. In the stationary phase, however, HU could facilitate bacterial cell death, resulting in widespread dissolution of EcSSB condensates.

Unlike exponential-phase cells, stationary-phase cells retained up to 70 % of their EcSSB-GFP signal in the condensate form. However, in the presence of stressors including glucose, H_2O_2, HU, and UV, this value often dropped below 40 %. In addition, diamide exhibited a reduced propensity to induce localization of condensates near the membrane compared to that seen in the exponential phase, while UV occasionally promoted such localization (**Figs. 2 and 3**). The latter effect was not detectable in exponential-phase experiments, as UV completely dissociated EcSSB droplets in that phase (**Fig. 2**). Nonetheless, this UV-induced behavior was less pronounced in the stationary phase compared to diamide during the exponential phase. Together, these observations demonstrate that stationary-phase cells, exhibiting slower metabolism and lower demand for rapid DNA replication, show reduced sensitivity to stressors with respect to EcSSB condensation.

The subcellular localization of EcSSB underwent significant changes in the death phase (**Fig. S2 and Table S5**), with condensates becoming barely visible and only a faint cytoplasmic signal remaining. This phenomenon may occur because cells begin to reutilize their resources, while also degrading their EcSSB pool. Most stressors, except for NaCl, diamide, and nitrofurantoin, exerted minimal influence on EcSSB localization during this phase. These specific molecules

promote the formation of small condensates, potentially by inducing osmotic stress, which could lead to locally elevated protein concentrations, thereby promoting droplet formation.

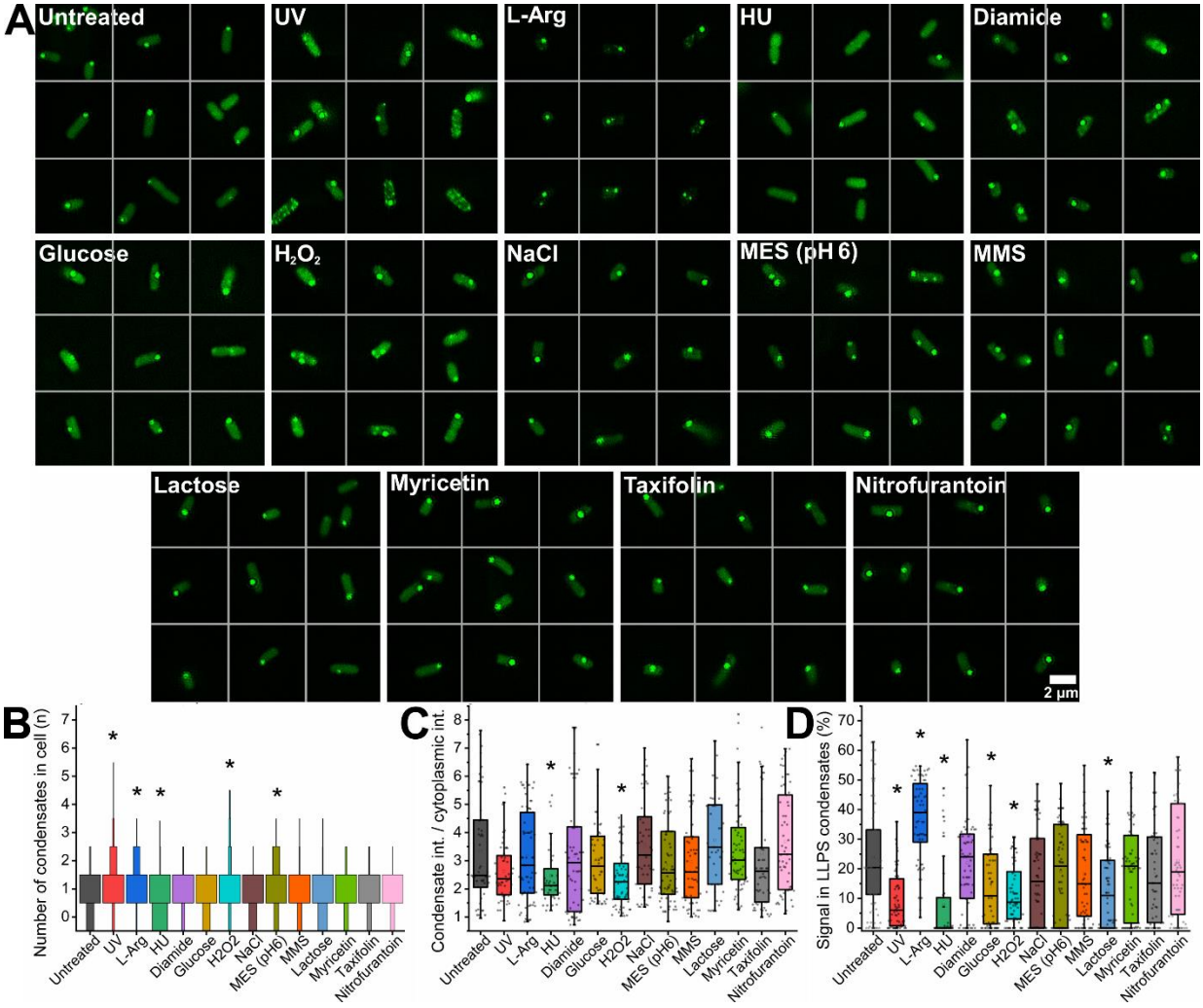

Figure 3. Stress-induced EcSSB decondensation is attenuated in stationary growth phase (OD_{600} = 0.6 + 3 h). (A) *Representative SIM images of E. coli strain #29003 show one bright focus in each cell, indicating EcSSB accumulation into a single large condensate. Stressors affected EcSSB-GFP patterns to a markedly lesser extent than in exponential-phase cells (OD_{600} = 0.6,* ***Fig. 2****; see* ***Table S2*** *for conditions). However, UV, MES (pH 6), H_2O_2, and glucose remained the most effective disruptors of EcSSB condensates. Analysis of* ***(B)*** *the number and* ***(C)*** *intensity of foci in cells showed that stressors causing DNA damage (e.g. UV and H_2O_2) elicit a rapid response initiating the fragmentation of EcSSB droplets, while glucose (presumed to restart cell growth over time) causes the droplets to slowly dissociate.* ***(D)*** *Cells contained markedly higher percentages of EcSSB in condensates compared to cells in earlier phases (OD_{600} = 0.2 and 0.6,* ***Figs. 1-2****). Asterisks denote significant difference compared to untreated cells (Mann-Whitney test, $p < 0.05$, n = 65 cells analyzed per condition, see also* ***Table S4****.*

EcSSB relocalizes to DNA-rich regions through stress-induced condensate dissolution

We previously demonstrated that ssDNA exerts an inhibitory effect on EcSSB condensation *in vitro* [9]. This observation raised the possibility that bacterial DNA (nucleoid regions) and EcSSB condensates do not colocalize in the cytoplasm in the absence of stress. To test this proposition and define the spatial relationship between DNA and EcSSB assemblies in cells, we used Hoechst

33342 DNA dye and analyzed cells during exponential and stationary growth phases (**Fig. 4**). Indeed, we found that EcSSB-GFP condensates and Hoechst signals were spatially separated in both growth phases, with the separation being more pronounced during the stationary phase. These findings provide evidence for separate localization of EcSSB condensates and nucleoid regions in the cytoplasm, especially when cells are in a resting state with less intense DNA metabolism. This result further corroborates the sequestering function of EcSSB condensates in stress-free physiological states.

Importantly, when H_2O_2 and MES (pH 6) were applied (selected based on the above results as effective stressors), the dissolution of EcSSB-GFP condensates was accompanied by a higher level of association between DNA and EcSSB-GFP signals (**Fig. 4**). These findings provide evidence for stress-induced DNA association of EcSSB *in vivo*, occurring through rapid dissolution of EcSSB condensates, as we proposed earlier based on EcSSB's *in vitro* condensation features [9].

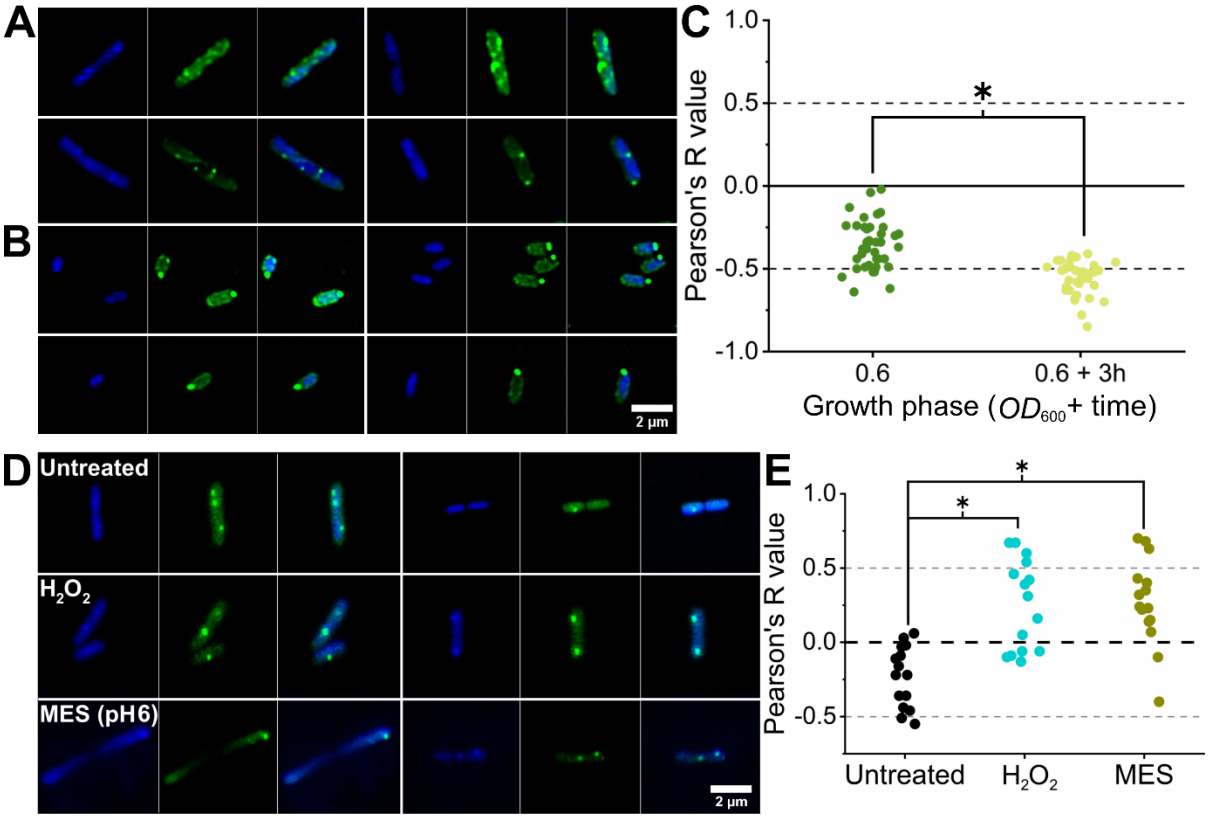

Figure 4. Physiological EcSSB sequestration from, and stress-induced association to cellular DNA. *Shown are SIM images of Hoechst 33342-stained (blue) E. coli #29003 cells (EcSSB-GFP, green) in the* ***(A)*** *exponential (OD_{600} = 0.6) and* ***(B)*** *stationary (OD_{600} = 0.6 + 3 h) growth phases.* ***(C)*** *Pearson's analysis of EcSSB-GFP and Hoechst signals shows marked anticorrelation in the exponential phase, which is significantly enhanced in the stationary phase in which genome maintenance processes are less intense (Mann-Whitney test, $p < 0.05$). These results support that EcSSB droplets function to sequester EcSSB from DNA during periods of lower genome metabolic demand.* ***(D)*** *Confocal microscopic images showing Hoechst 33342-stained (blue) E. coli #29003 cells (EcSSB-GFP, green) in the exponential growth phase (OD_{600} = 0.6) in the absence and presence of stressors (see* ***Table S2*** *for conditions).* ***(E)*** *Pearson's analysis of EcSSB-GFP and Hoechst signals shows the association of EcSSB with DNA under stress (Mann-Whitney test, $p < 0.05$). Note that DNA accumulates to a higher extent in larger protein droplets.*

*This step presumably precedes the complete disassembly of condensates. Cells with H_2O_2 and MES treatment contained a smaller number of foci compared to stress-free cells, as was also seen in **Fig. 2**.*

In vitro **assays demonstrate physicochemical plausibility of the EcSSB liquid condensate-based cellular regulation mechanism**

In addition to our *in vivo* experiments (**Figs. 1-4 and S1-2**), we carried out a comprehensive array of well-controlled *in vitro* biophysical measurements on EcSSB condensates to provide a quantitative framework that links droplet-level morphologies across isolated molecular systems and cellular organization (**Figs. S3-S6**). These *in vitro* fluorescence microscopic, turbidity-based, microscale thermophoresis (MST), microfluidic resistive pulse sensing (MRPS), and dynamic light scattering (DLS) experiments revealed that (*i*) EcSSB condensation during exponential growth indeed can arise from protein concentrations surpassing a critical LLPS threshold, (*ii*) that cellular EcSSB droplets represent *bona fide* LLPS assemblies, and that (*iii*) the applied stressors indeed modulate EcSSB condensates through cellular response mechanisms.

First, we probed the chemical sensitivity of EcSSB droplets to condensation effectors **(Fig. S3)**. We found that the aliphatic alcohol 1,6-hexanediol, a well-established LLPS inhibitor [34], showed characteristic inhibition of EcSSB droplet formation at high concentrations (> 300 mM). The effective range of 1,6-hexanediol was similar to that observed earlier for condensation of the human SSB2 homolog [35]. Phase-separating proteins have been shown to effectively form condensates under conditions with reduced water potential [21]. Therefore, we assessed EcSSB condensation at increasing concentrations of sorbitol, an agent suitable to monitor LLPS under a broad range of osmotic conditions. EcSSB underwent phase separation even at 500 mg/ml sorbitol (**Fig. S3C-D**), which exceeds the macromolecule concentration in an osmotically stressed bacterial cytoplasm [36], indicating that EcSSB can perform its condensation-dependent functions even in osmotically stressed bacteria. The reduction in EcSSB condensation at extremely high sorbitol concentrations (> 500 mg/ml) probably originated from the increased viscosity of the medium (**Fig. S3C-D**). Moreover, we found that the organic solvent DMSO exhibited notable inhibitory effects on EcSSB condensation only at high concentrations (> 8 v/v%), highlighting the resilient nature of EcSSB condensates in the presence of organic solvents (**Fig. S3E-F**). This result also verifies that DMSO, as a small molecule solvent, is suitable for future applications screening small-molecule active substances for effects on EcSSB condensation.

Next, we performed *in vitro* microscale thermophoresis (MST) experiments to describe the concentration-dependent onset and time scale of EcSSB condensate formation **(Fig. S4)**. These measurements revealed that the critical EcSSB concentration for phase transition (2.5 μM) is below the physiological EcSSB concentration **(Fig. S4A-B)** [37]. Moreover, we found that the condensation response of EcSSB is rapid (extensive condensation was already observed at 2 minutes after reaction onset), and the data reflected subsequent particle growth in the minutes time scale **(Fig. S4C-D)**. The NaCl concentration-dependent inhibition profile of the MST response was in line with the well-established chloride inhibition feature of EcSSB condensation [9-11,24], corroborating that the MST curves monitor *bona fide* protein LLPS processes **(Fig. S4E-F)**.

We defined the size distribution of individual EcSSB condensate particles *in vitro* by microfluidic resistive pulse sensing (MRPS) experiments **(Fig. S5)**. These measurements revealed lognormal

size distributions for EcSSB condensates that scaled with protein concentration. This behavior provides additional evidence for the liquid nature of EcSSB condensates, while the condensate size scaling defined *in vitro* also parallels droplet size variabilities observed *in vivo* (**Figs. 1-4**). In addition, our time-dependent dynamic light scattering (DLS) measurements of the hydrodynamic radius of EcSSB condensates provided evidence for rapid formation of EcSSB condensates with moderate growth on slower time scales **(Fig. S6A)**. We found that polydispersity decreases with EcSSB concentration, reinforcing condensate maturation/coalescence occurring at higher EcSSB concentrations **(Fig. S6B)**, in line with condensate dynamics observed *in vivo* across growth phases (**Fig. 1**). Together, the above *in vitro* findings (**Figs. S3-S6**) establish EcSSB condensation as a rapid, protein concentration-dependent, and tunable process that mirrors the behavior observed *in vivo* across growth phases and under stress (**Figs. 1-4**).

Stressors modulate EcSSB condensates through cellular response mechanisms

To define the direct effects of the stressors applied *in vivo* (**Figs. 2-4**) on EcSSB condensation *in vitro*, turbidity assays (λ = 600 nm) were conducted alongside epifluorescence imaging of purified EcSSB samples **(Fig. S7)**. The results revealed that most of the applied stressors do not influence the formation of EcSSB condensates *in vitro*, even at high stressor concentrations. Notably, despite the previously defined inhibitory effect of NaCl on EcSSB condensation *in vitro* [9,11], this agent even enhanced condensate formation *in vivo* (**Fig. 2**). Besides NaCl, L-Arg was the only effector that exhibited marked EcSSB condensation inhibition *in vitro* at the dose applied *in vivo*. The presence of spherical, phase-separated droplets in epifluorescence microscopic images demonstrates that the turbidity signals originate from LLPS rather than amorphous protein aggregation in the case of most applied stressors. Taken together, these results demonstrate that the effects observed *in vivo* are mediated through cellular response mechanisms impacting EcSSB condensates.

Discussion

Recent discoveries on liquid-liquid phase separation (LLPS) have transformed our understanding of cellular organization in eukaryotes. In contrast, the role of LLPS in bacteria remains poorly understood, despite growing evidence suggesting that phase transition processes play central roles in bacterial stress adaptation and post-stress resuscitation [17,38]. How bacterial cells detect and respond to stress—and whether LLPS constitutes a mechanistic basis for these processes—remains a fundamental scientific question. In this work, we provide evidence for a dynamic condensation mechanism of *Escherichia coli* single-stranded DNA-binding protein (EcSSB), combining *in vivo* super-resolution microscopy with a comprehensive array of *in vitro* biophysical measurements. Our current findings demonstrate that EcSSB undergoes condensation in bacterial cells under stress-free conditions and that these condensates are spatially separated from DNA (**Figs. 1** and **4**). Notably, slower metabolic rates correlate with the formation of larger condensates. Importantly, EcSSB condensates dissolve or fragment in response to various stressors and metabolic shifts, which also trigger increased association of EcSSB with DNA (**Figs. 2** and **4**). Results from previous *in vitro* studies suggested a potential mechanism for condensate dissolution. ssDNA was shown to become enriched within EcSSB condensates and bind to the tetramers. This binding, however, competes with the multivalent interactions that drive EcSSB phase separation. Once the ssDNA concentration reaches a critical threshold, this competition is sufficient to initiate condensate dissolution, ultimately leading to

complete disassembly [9,11,24]. In the cytoplasm, this process may be promoted by increasing concentrations of genomic ssDNA stretches during stress or elevated metabolic activity. This is also consistent with our *in vivo* observations of spatial separation between DNA and EcSSB condensates when the ssDNA concentration is low, and increased EcSSB-DNA association in stress states (**Fig. 4**).

An important question raised by our findings concerns the physiological consequences of impaired EcSSB phase separation. Here we propose that LLPS of EcSSB functions as a buffering and mobilization system that regulates the availability of ssDNA binding capacity in bacterial cells. If EcSSB were unable to undergo LLPS, the cellular distribution of the protein would be expected to shift toward a constitutively diffuse cytoplasmic pool with an increased concentration. This could lead to unproductive protein-DNA interactions during transcription or replication, potentially interfering with replication fork dynamics or the coordination of DNA repair. To maintain genome integrity, bacteria may therefore reduce the overall concentration of EcSSB, which could result in delayed responses to DNA damage. Consistent with this view, Bond *et al.* found that bacteria expressing only a variant of EcSSB lacking the IDL (but retaining the CTP, SSBΔ120–166), which is known to be less effective to form LLPS droplets [10], contained about half the amount of EcSSB compared to the WT strain (~8800 ± 2700 monomers of SSBΔ120–166 *versus* 19700 ± 5600 monomers of WT per cell) [5]. In the current study we observed EcSSB foci with diameters typically ranging from 100–500 nm. Based on the crystal structure of EcSSB (PDB: 4MZ9) in which EcSSB forms a tetrameric assembly with a ~50 Å diameter, a few thousand tetramers packed in a crystalline-like arrangement would result in such condensate sizes. This amount is consistent with the mentioned difference between WT and mutant EcSSB protein levels. However, we note that this estimation does not account for differences in packing density between crystals and LLPS droplets, the structural effects of EcSSB's intrinsically disordered tail region, and the possible incorporation of EcSSB's interacting partners, all of which could influence condensate size *in vivo*.

In addition to the above considerations, we previously showed that RecQ helicase, one of EcSSB's key interacting partners, becomes enriched within EcSSB condensates *in vitro*, suggesting co-sequestration of genome maintenance factors *in vivo* [9,24]. Thus, the loss of EcSSB's LLPS propensity could also affect the available concentrations of other DNA maintenance proteins for the same reasons. Moreover, these associated proteins are presumably released in a coordinated manner with EcSSB upon stress-induced dissolution of condensates. Disruption of EcSSB-driven spatial organization could impair this coordinated release and, consequently, compromise the efficiency of DNA repair processes. In addition, sequestration could protect sensitive factors from degradation, reducing energy consumption and enhancing survival.

Beyond stress adaptation, the observations presented here support an emerging view of prokaryotic material organization mechanisms involving dynamic protein condensation [21,39-41]. Global cytoplasmic transitions in bacteria from fluid-like to glass-like states have been reported in response to decreased metabolic activity [21], and metabolism-driven cytoplasmic fluidization has been linked to enhanced molecular mobility [21,42]. Our findings on growth phase and metabolism dependent EcSSB condensation suggest that the discovered mechanism contributes to these broader cytoplasmic phase transitions during metabolic shifts and adaptation.

Our findings suggest that EcSSB's condensation propensity confers a selective advantage to bacteria during fluctuating environmental conditions *via* enhanced stress survival and faster responses to metabolic changes. The effects of condensation could affect survival on longer time

scales and become more pronounced under competitive conditions. Compromised condensation propensity might affect genome stability, as supported by previous findings showing that cells expressing EcSSB tetramers with only two IDLs, presumably with reduced LLPS propensity and partner binding capacity, exhibit increased mutation rates [43]. Nonetheless, an elevated mutational burden could, under certain conditions such as antibiotic exposure, facilitate the emergence of resistance to antimicrobial agents over shorter timescales. Testing these hypotheses and determining the phenotypic consequences of altered condensation propensity will require extended investigations using genetically engineered EcSSB variants that are incapable of undergoing LLPS while retaining their ssDNA-binding function [24]. Such studies are beyond the scope of the present work, but our results highlight directions for future research. In **Figure 5** we integrate current knowledge on the relationship between *in vitro* effectors and *in vivo* regulation of EcSSB condensation dynamics.

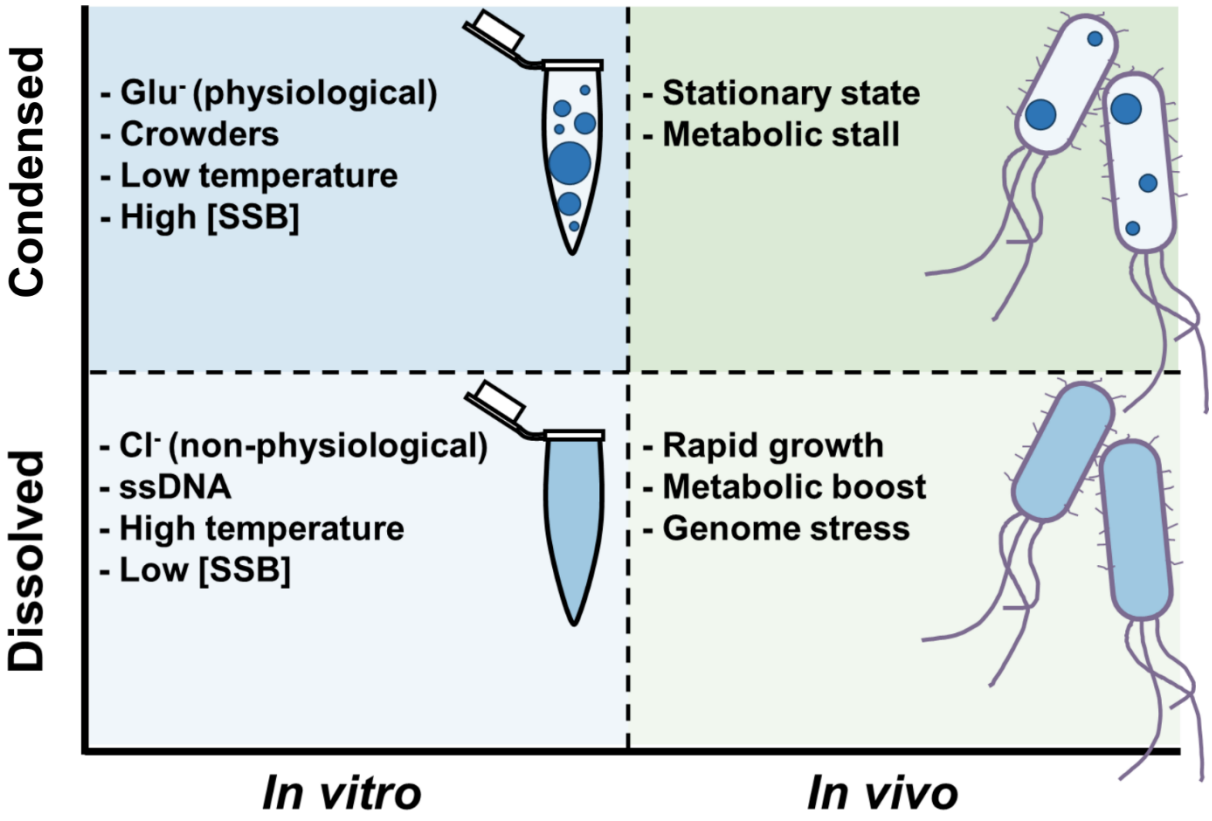

Figure 5. "Phase map" of EcSSB. *EcSSB condensates are highly dynamic structures whose formation and dissolution is regulated by multiple factors both in vitro [9,11,24] and in vivo (this paper). This responsiveness allows EcSSB condensates to function as efficient tools for bacterial cells, facilitating the sequestration of proteins when not required and enabling their rapid mobilization to sites of action upon demand. Note that in vitro conditions mimicking the unstressed cellular environment promote condensation.*

Finally, we emphasize that the imaging analysis pipeline defined in the current study (**Supplementary file 1**) constitutes a valuable tool for the broader study of LLPS *in vivo* by enabling quantitative assessment of condensate properties in diverse genetic or environmental contexts. Taken together, our work positions EcSSB condensation as a dynamic and tunable component of bacterial DNA metabolic regulation. Hence, these insights can also open potential avenues for antimicrobial discovery by targeting phase separation pathways.

Materials and Methods

Materials

Stressors used in this study, including their applied dose and mechanism of action, are described in detail in **Table S2**. In this work we used an *E. coli* strain #29003, which was a kind gift from Piero R. Bianco [23]. Note that, the WT protein also present in these bacteria thus the GFP fused protein can only be used as a marker to follow EcSSB condensates. Recombinant EcSSB expression and purification, as well as AF555 (AlexaFluor 555) and IAF (5-iodoacetamidofluorescein) labeling was carried out as described in Harami *et al.* [9] Since EcSSB does not contain any cysteines, the $EcSSB^{G26C}$ variant was used for IAF labeling. AF555 labeling was performed on wild type EcSSB. EcSSB protein concentrations are expressed in terms of EcSSB tetramers throughout this article.

Cell culture preparation for fluorescence imaging

Cells were grown overnight in Luria–Bertani medium (LB) containing kanamycin (25 µg/ml) and chloramphenicol (34 µg/ml) at 37°C. Overnight cultures were diluted 1:100 in fresh LB media containing antibiotics and grown at room temperature at 200 rpm shaking until they reached a certain OD_{600} value + time indicating the different growth phases (exponential, stationary or death phase). We note that room temperature was used to aid the maturation of GFP, thus enhancing the signal during imaging. During the exponential growth phase, the cultures exhibited a doubling time of approximately 45 minutes at this temperature. Cells were centrifuged, washed with 10 mM $MgSO_4$ twice, then resuspended in $MgSO_4$ containing the stressors at concentrations indicated in **Table S2**. The pH of stressor solutions was adjusted to 7.0 except for MES (pH 6) when necessary. Cells were shaken for 30 minutes at 200 rpm at 37 °C and subsequently imaged without any fixation or L-lysine treatment. Depending on cell density, dilutions were applied before imaging to avoid a confluence of cells during imaging. Notably, when cells in different growth phases were studied, no incubation in $MgSO_4$ was used, and they appeared identical to the untreated cells in the stress panels. This indicates that a 30-minute incubation in $MgSO_4$ does not significantly alter EcSSB condensate patterns. UV-stressed cells were also observed without incubation to avoid regeneration.

Super-resolution (SIM) and confocal microscopy of *E. coli* cells

For SIM microscopy, Zeiss High Performance 0.17 ± 0.005 mm thick glass coverslips and a Zeiss Elyra S1 SIM microscope with 488-nm (Lasos) laser were used. Hoechst 33342 (Biotium, #40046) DNA stain images were captured using a Nikon X-Light V3 Deep SIM microscope (LED, solid state from Lumencor). Cells were treated with Hoechst for one minute followed by two wash steps before observation. No noticeable changes in cell morphology and condensate patterns were observed between stained and unstained cells (*cf.* **Figs. 1** and **4**), demonstrating that the cells remained viable upon staining.

For confocal microscopy, a Zeiss LSM710 microscope was used with Menzel-Glaser (20x20 mm, Thermo scientific) glass cover slides. Hoechst 33342 staining was performed as described for SIM imaging.

Evaluation of microscopic images of *E. coli* cells

Image analysis was performed using Fiji software. To ensure accurate quantification, the brightest foci were checked for signal saturation, and no evidence of saturation or clipping

artifacts was found. For image evaluation purposes, two scripts were developed for a more automatic quantification of protein condensates in cells **(Supplementary file 1)**. During evaluation, cell segmentation was performed using Li cross-entropy thresholding, which determines the optimal intensity cutoff by minimizing cross-entropy. This method is robust for asymmetric and noisy intensity distributions, making it well-suited for automatic detection of cells in fluorescence images. This step was followed by another thresholding step within the cells to identify foci (condensates) using a modified Find Maxima function (**Fig. S8, Supplementary file 1**). A 2D Gaussian was fitted to each spot, and intensities were calculated by measuring the space under the Gaussian curve and correcting with the background at the base of the curves. The script can be fine-tuned at this step, as the Find Maxima function allows adjustment of the minimum intensity required for spot detection relative to the background. For the current study, the parameters were set based on untreated cells and applied identically to all treated samples to allow direct comparison. To determine the percentage of fluorescent signal present in the condensates compared to the cytoplasm, the developed script (**Supplementary file 1**) was used to outline condensates and to subtract them from the original image. The difference between intensities was used to define material percentage within condensates (**Fig. S1**). Although bacteria exhibited some autofluorescence in the GFP channel, this contribution was consistent across all samples, allowing reliable comparative analysis without further correction. Colocalization analysis of images of Hoechst-stained cells was performed using Fiji plugin Coloc2. To test the effect of the FM 4-64 membrane dye at different concentrations, the dye was applied at 2 µM and 8 µM (**Fig. S9**). In addition, we compared unprocessed and processed SIM images to visualize the resolution gain provided by the SIM technique (**Fig. S10**).

General measurement conditions for *in vitro* experiments

In vitro measurements were performed at 25°C in LLPS buffer containing 20 mM Tris-acetate (Tris-OAc) pH 7.5, 5 mM MgOAc and 50 mM NaGlu.

Turbidity assays of purified EcSSB condensates

Turbidity measurements were performed at 600 nm, using Thermo Fisher Nunc 384-well, non-treated flat bottom microplates and a Tecan Infinite F Nano+ plate reader instrument. The sample volume was 100 µL, in a buffer containing 20 mM Tris-OAc pH 7.5, 5 mM MgOAc and 50 mM NaGlu. The EcSSB tetramer concentration was 5 µM. Measurements were performed in triplicate at room temperature.

Epifluorescence microscopy of purified EcSSB condensates

The effects of stressors on EcSSB condensates *in vitro* were visualized using epifluorescence microscopy. Samples contained 5 µM EcSSB tetramers and 0.1 µM fluorescein-labeled EcSSB, which readily became enriched in EcSSB droplets [9]. Samples were measured on Ibidi 15 Well µ-Slide Angiogenesis slides at room temperature. A Nikon Eclipse Ti-E TIRF microscope was used in epifluorescence mode with a Cyan 488-nm laser (Coherent). Determination of total droplet area in middle ROI was carried out as in [44].

Microscale thermophoresis (MST)

The thermophoretic mobility of 5 µM EcSSB (containing 50 nM iodoacetamidofluorescein (IAF)-labeled $EcSSB^{G26C}$) was monitored using a Nanotemper Monolith device (set to 20 % MST power and 75 % excitation power) in LLPS buffer. Premium capillaries were used for sample

loading. Capillary scans showed ideal capillary shapes and no protein adhesion to the surface. Baseline was recorded for 5 seconds before infrared irradiation for 30 seconds. Fluorescence recovery was monitored for additional 5 seconds after the end of irradiation. Fluorescence was normalized to baseline. Thermophoretic mobility was determined as the fraction of the baseline fluorescence signal (F_{norm}) measured at 20 seconds irradiation.

Microfluidic resistive pulse sensing (MRPS)

MRPS measurements were performed using an nCS1 instrument (Spectradyne LLC, USA). Data obtained were analysed using Viewer software (Spectradyne LLC, USA). EcSSB was diluted in LLPS buffer unless otherwise indicated. Samples were measured using a C-2000 cartridge (~250 nm to 2000 nm measurement range).

Dynamic light scattering (DLS)

EcSSB samples were diluted in LLPS buffer and measured in low volume disposable cuvettes with 1 cm path-length (UVette, Eppendorf Austria GmbH) using a W130i dynamic light scattering device (DLS, Avid Nano Ltd., High Wycombe, UK) equipped with a diode laser (660 nm) and a photodiode detector.

Data Availability

The data underlying this article are available in the article and in its online Supplementary Material. The data underlying this article will be shared upon reasonable request to the corresponding author.

Supplementary Data

Supplementary Data are provided with this article.

Author Contributions

P.E.: Conceptualization, Data curation, Formal Analysis, Investigation, Methodology Validation, Visualization, Writing – original draft, Writing – review & editing, Funding acquisition. **J.S.**: Investigation, Data curation, Validation, Writing – original draft. **J.P.**: Investigation, Methodology. **B.J.**: Conceptualization, Methodology. **V.K.**: Investigation. **Z.J.K.**: Investigation. **H.H.**: Investigation, Methodology. **T.S.**: Investigation. **T.J.**: Investigation, Methodology. **T.B.S.**: Conceptualization, Methodology. **S.B.**: Investigation, Methodology. **E.S.M.**: Investigation, Methodology. **M.K.**: Conceptualization, Funding acquisition, Project administration, Resources, Supervision, Writing – review & editing. We thank Gábor M. Harami for insightful discussions in the topic of the manuscript.

Funding

This work was supported by grants ELTE KMOP-4.2.1/B-10-2011-0002, NKFIH K-123989, NKFIH K-134595, and NKFIH ADVANCED 150087 to M.K., and NKFIH PD-146123 to P.E. The project was supported by the NRDIO (VEKOP-2.3.3-15-2016-00007) grant to ELTE. P.E. and J.P. were supported by the EKÖP-24 university excellence scholarship program (EKÖP-24-4-IIELTE-92 and EKÖP-24-4-I-ELTE-184, respectively) of the Hungarian Ministry for Culture and Innovation from the source of the National Research, Development and Innovation Fund. P.E. is a holder of the Bolyai Research Fellowship of the Hungarian Academy of Sciences [BO/00566/24]. J.P. was supported by the Cooperative Doctoral Program of the Ministry of Innovation and Technology financed from the National Research, Development and Innovation

Fund. This work was completed in the framework of Project no. 2018-1.2.1-NKP-2018-00005 implemented with the support provided from the National Research, Development and Innovation Fund of Hungary, financed under the 2018-1.2.1-NKP funding scheme. Funded by the European Union HORIZON WIDERA 2023 IDP2Biomed grant agreement No. 101160233. Views and opinions expressed are however those of the author(s) only and do not necessarily reflect those of the European Union or the European Research Executive Agency (REA). Neither the European Union nor the granting authority can be held responsible for them. This research is carried out and financed within the framework of the second Swiss Contribution MAPS. SIM measurements were performed in the Nano-Bio-Imaging core facility at the University of Pécs. This project has received funding from the HUN-REN Hungarian Research Network.

Conflict of Interest

The authors have no conflicts of interest to declare.

References

1 Chatterjee, N. & Walker, G. C. Mechanisms of DNA damage, repair, and mutagenesis. *Environmental and molecular mutagenesis* **58**, 235-263, doi:10.1002/em.22087 (2017).
2 Shereda, R. D., Kozlov, A. G., Lohman, T. M., Cox, M. M. & Keck, J. L. SSB as an organizer/mobilizer of genome maintenance complexes. *Critical reviews in biochemistry and molecular biology* **43**, 289-318, doi:10.1080/10409230802341296 (2008).
3 Bonde, N. J., Kozlov, A. G., Cox, M. M., Lohman, T. M. & Keck, J. L. Molecular insights into the prototypical single-stranded DNA-binding protein from E. coli. *Critical reviews in biochemistry and molecular biology* **59**, 99-127, doi:10.1080/10409238.2024.2330372 (2024).
4 Raghunathan, S., Kozlov, A. G., Lohman, T. M. & Waksman, G. Structure of the DNA binding domain of E. coli SSB bound to ssDNA. *Nature structural biology* **7**, 648-652, doi:10.1038/77943 (2000).
5 Bonde, N. J., Henry, C., Wood, E. A., Cox, M. M. & Keck, J. L. Interaction with the carboxy-terminal tip of SSB is critical for RecG function in E. coli. *Nucleic acids research* **51**, 3735-3753, doi:10.1093/nar/gkad162 (2023).
6 Dubiel, K. *et al.* Development of a single-stranded DNA-binding protein fluorescent fusion toolbox. *Nucleic acids research* **48**, 6053-6067, doi:10.1093/nar/gkaa320 (2020).
7 Antony, E. & Lohman, T. M. Dynamics of E. coli single stranded DNA binding (SSB) protein-DNA complexes. *Seminars in cell & developmental biology* **86**, 102-111, doi:10.1016/j.semcdb.2018.03.017 (2019).
8 Shereda, R. D., Reiter, N. J., Butcher, S. E. & Keck, J. L. Identification of the SSB binding site on E. coli RecQ reveals a conserved surface for binding SSB's C terminus. *Journal of molecular biology* **386**, 612-625, doi:10.1016/j.jmb.2008.12.065 (2009).
9 Harami, G. M. *et al.* Phase separation by ssDNA binding protein controlled via protein-protein and protein-DNA interactions. *Proceedings of the National Academy of Sciences of the United States of America* **117**, 26206-26217, doi:10.1073/pnas.2000761117 (2020).
10 Kozlov, A. G. *et al.* How Glutamate Promotes Liquid-liquid Phase Separation and DNA Binding Cooperativity of E. coli SSB Protein. *Journal of molecular biology* **434**, 167562, doi:10.1016/j.jmb.2022.167562 (2022).
11 Kovacs, Z. J. *et al.* Fine-tuned interactions between globular and disordered regions of single-stranded DNA binding (SSB) protein are required for dynamic condensation under physiological conditions. *Protein science : a publication of the Protein Society* **34**, e70109, doi:10.1002/pro.70109 (2025).
12 Guo, D. *et al.* Liquid-Liquid phase separation in bacteria. *Microbiological research* **281**, 127627, doi:10.1016/j.micres.2024.127627 (2024).
13 Uversky, V. N. Biological Liquid-Liquid Phase Separation, Biomolecular Condensates, and Membraneless Organelles: Now You See Me, Now You Don't. *International journal of molecular sciences* **24**, doi:10.3390/ijms241713150 (2023).
14 Tong, X. *et al.* Liquid-liquid phase separation in tumor biology. *Signal transduction and targeted therapy* **7**, 221, doi:10.1038/s41392-022-01076-x (2022).
15 Peng, P. H., Hsu, K. W. & Wu, K. J. Liquid-liquid phase separation (LLPS) in cellular physiology and tumor biology. *American journal of cancer research* **11**, 3766-3776 (2021).
16 Wang, B. *et al.* Liquid-liquid phase separation in human health and diseases. *Signal transduction and targeted therapy* **6**, 290, doi:10.1038/s41392-021-00678-1 (2021).
17 Jin, X. *et al.* Membraneless organelles formed by liquid-liquid phase separation increase bacterial fitness. *Science advances* **7**, eabh2929, doi:10.1126/sciadv.abh2929 (2021).
18 Gomes, E. & Shorter, J. The molecular language of membraneless organelles. *The Journal of biological chemistry* **294**, 7115-7127, doi:10.1074/jbc.TM118.001192 (2019).
19 Poudyal, M. *et al.* Intermolecular interactions underlie protein/peptide phase separation irrespective of sequence and structure at crowded milieu. *Nature communications* **14**, 6199, doi:10.1038/s41467-023-41864-9 (2023).
20 Feng, Z., Chen, X., Wu, X. & Zhang, M. Formation of biological condensates via phase separation: Characteristics, analytical methods, and physiological implications. *The Journal of biological chemistry* **294**, 14823-14835, doi:10.1074/jbc.REV119.007895 (2019).
21 Azaldegui, C. A., Vecchiarelli, A. G. & Biteen, J. S. The emergence of phase separation as an organizing principle in bacteria. *Biophysical journal* **120**, 1123-1138, doi:10.1016/j.bpj.2020.09.023 (2021).
22 Alberti, S., Gladfelter, A. & Mittag, T. Considerations and Challenges in Studying Liquid-Liquid Phase Separation and Biomolecular Condensates. *Cell* **176**, 419-434, doi:10.1016/j.cell.2018.12.035 (2019).
23 Zhao, T. *et al.* Super-resolution imaging reveals changes in Escherichia coli SSB localization in response to DNA damage. *Genes to cells : devoted to molecular & cellular mechanisms* **24**, 814-826, doi:10.1111/gtc.12729 (2019).
24 Ecsedi, P. *et al.* Selective engineering of condensation properties of single-stranded DNA binding (SSB) protein via its intrinsically disordered linker region. *Nucleic acids research* **53**, doi:10.1093/nar/gkaf481 (2025).
25 Liu, J. *et al.* Novel, fluorescent, SSB protein chimeras with broad utility. *Protein science : a publication of the Protein Society* **20**, 1005-1020, doi:10.1002/pro.633 (2011).
26 Ulbrich, M. H. & Isacoff, E. Y. Subunit counting in membrane-bound proteins. *Nature methods* **4**, 319-321, doi:10.1038/nmeth1024 (2007).
27 Kram, K. E., Henderson, A. L. & Finkel, S. E. Escherichia coli Has a Unique Transcriptional Program in Long-Term Stationary Phase Allowing Identification of Genes Important for Survival. *mSystems* **5**, doi:10.1128/mSystems.00364-20 (2020).
28 Schink, S. J., Biselli, E., Ammar, C. & Gerland, U. Death Rate of E. coli during Starvation Is Set by Maintenance Cost and Biomass Recycling. *Cell systems* **9**, 64-73 e63, doi:10.1016/j.cels.2019.06.003 (2019).

29 Lin, E. S., Huang, Y. H., Luo, R. H., Basharat, Z. & Huang, C. Y. Crystal Structure of an SSB Protein from Salmonella enterica and Its Inhibition by Flavanonol Taxifolin. *International journal of molecular sciences* **23**, doi:10.3390/ijms23084399 (2022).
30 Lin, E. S., Luo, R. H. & Huang, C. Y. A Complexed Crystal Structure of a Single-Stranded DNA-Binding Protein with Quercetin and the Structural Basis of Flavonol Inhibition Specificity. *International journal of molecular sciences* **23**, doi:10.3390/ijms23020588 (2022).
31 Nazaretyan, S. A. *et al.* Replication Rapidly Recovers and Continues in the Presence of Hydroxyurea in Escherichia coli. *Journal of bacteriology* **200**, doi:10.1128/JB.00713-17 (2018).
32 Liu, L. *et al.* Changes in intra-nuclear mechanics in response to DNA damaging agents revealed by time-domain Brillouin micro-spectroscopy. *Photoacoustics* **27**, 100385, doi:10.1016/j.pacs.2022.100385 (2022).
33 Li, Y. *et al.* Versatile cell-based assay for measuring DNA alkylation damage and its repair. *Scientific reports* **11**, 18393, doi:10.1038/s41598-021-97523-w (2021).
34 Duster, R., Kaltheuner, I. H., Schmitz, M. & Geyer, M. 1,6-Hexanediol, commonly used to dissolve liquid-liquid phase separated condensates, directly impairs kinase and phosphatase activities. *The Journal of biological chemistry* **296**, 100260, doi:10.1016/j.jbc.2021.100260 (2021).
35 Kovacs, Z. J. *et al.* DNA-dependent phase separation by human SSB2 (NABP1/OBFC2A) protein points to adaptations to eukaryotic genome repair processes. *Protein science : a publication of the Protein Society* **33**, e4959, doi:10.1002/pro.4959 (2024).
36 van den Bogaart, G., Hermans, N., Krasnikov, V. & Poolman, B. Protein mobility and diffusive barriers in Escherichia coli: consequences of osmotic stress. *Molecular microbiology* **64**, 858-871, doi:10.1111/j.1365-2958.2007.05705.x (2007).
37 Bobst, E. V., Bobst, A. M., Perrino, F. W., Meyer, R. R. & Rein, D. C. Variability in the nucleic acid binding site size and the amount of single-stranded DNA-binding protein in Escherichia coli. *FEBS letters* **181**, 133-137, doi:10.1016/0014-5793(85)81128-5 (1985).
38 Ladouceur, A. M. *et al.* Clusters of bacterial RNA polymerase are biomolecular condensates that assemble through liquid-liquid phase separation. *Proceedings of the National Academy of Sciences of the United States of America* **117**, 18540-18549, doi:10.1073/pnas.2005019117 (2020).
39 Janissen, R. *et al.* Global DNA Compaction in Stationary-Phase Bacteria Does Not Affect Transcription. *Cell* **174**, 1188-1199 e1114, doi:10.1016/j.cell.2018.06.049 (2018).
40 Calhoun, L. N. & Kwon, Y. M. Structure, function and regulation of the DNA-binding protein Dps and its role in acid and oxidative stress resistance in Escherichia coli: a review. *Journal of applied microbiology* **110**, 375-386, doi:10.1111/j.1365-2672.2010.04890.x (2011).
41 Almiron, M., Link, A. J., Furlong, D. & Kolter, R. A novel DNA-binding protein with regulatory and protective roles in starved Escherichia coli. *Genes & development* **6**, 2646-2654, doi:10.1101/gad.6.12b.2646 (1992).
42 Parry, B. R. *et al.* The bacterial cytoplasm has glass-like properties and is fluidized by metabolic activity. *Cell* **156**, 183-194, doi:10.1016/j.cell.2013.11.028 (2014).
43 Antony, E. *et al.* Multiple C-terminal tails within a single E. coli SSB homotetramer coordinate DNA replication and repair. *Journal of molecular biology* **425**, 4802-4819, doi:10.1016/j.jmb.2013.08.021 (2013).
44 Harami, G. M. *et al.* Redox-dependent condensation and cytoplasmic granulation by human ssDNA-binding protein-1 delineate roles in oxidative stress response. *iScience* **27**, 110788, doi:10.1016/j.isci.2024.110788 (2024).